Pathways of structural and magnetic transition in ferromagnetic shape-memory alloys

Matthew R. Sullivan, Ashish A. Shah, and Harsh Deep Chopra*
Thin Films and Nanosynthesis Laboratory, Materials Program, Mechanical and Aerospace Engineering Department, SUNY-Buffalo, Buffalo, New York 14260, USA
(Received 12 December 2003; revised manuscript received 12 May 2004; published 30 September 2004)

A fundamental question in the study of ferromagnetic shape-memory alloys is, what is the nature of the magneto-elastic coupling in these alloys and to what extent does it drive the structural transformation? This question also holds the key to developing new and optimized alloys that combine high strains at low switching field. In the present study, it is shown that the reconfiguration of the micromagnetic structure is completely enslaved to and follows the martensitic structural transformation in these alloys, using Ni–Mn–Ga and Fe–Pd systems. This is determined by developing a new high-speed electronic method to study temperature-dependent domain dynamics, called "magnetic transition spectra." The sequence of structural and magnetic transitions was found to be as follows: Cooling: structural transition followed by micromagnetic reconfiguration; Heating: micromagnetic reconfiguration followed by structural transition.

DOI: 10.1103/PhysRevB.70.094428 PACS number(s): 75.80.+q

I. INTRODUCTION

Shape-memory alloys (SMAs) provide large displacements and forces within a small actuator design. However, these alloys have slow dynamic response due to temperature-controlled actuation. In recent years, an alternative approach to (faster) actuation has emerged through the use of SMAs that are ferromagnetic in nature.[1,2] Ferromagnetic shape-memory alloys (FSMAs) offer an ability to cause actuation by an applied magnetic field rather than the slow process of shape change by temperature, thereby combining high strains with fast reaction times. The FSMAs are complex correlated systems whose physical properties are governed by interactions across different energy regimes (thermal, magnetic, and elastic). These interactions produce a rich variety of phenomena, such as, for example, the magneto-elastic shape memory effect,[1,2] thermo-elastic shape memory effect,[3] and the magneto-caloric effect.[4] Examples of FSMAs include the Fe–Pd, Fe–Pt, Fe–Ni, Fe–Ni–Co–Ti, Co–Ni–Ga systems, and the family of Heusler alloys such as the $Ni_{2+x}Mn_{1-x}Ga$ system, which undergoes a reversible, thermo-elastic martensitic phase transformation.

The ferromagnetic Weiss domains in FSMAs are magneto-elastically coupled to and superimposed on the martensite structure. Due to this coupling, when the geometrical configuration of the magnetic domains is altered by an applied magnetic field, it also leads to a change in the relative volume fraction of the martensite twins,[5–8] thereby enabling field-induced shape change. Practical applications require large strains at low switching fields. The magnitude of the switching field, in turn, depends on the magneto-elastic coupling, which governs the magnitude of the applied field either to cause a structural transformation or change the relative volume fraction of martensite twins. It is widely recognized that the trial and error method of designing new alloys would give way to a more scientific approach if the transformation pathways of structural and magnetic transitions could be understood. Whereas the structural transition is the well-known displacive, diffusionless martensite transformation, the magnetic transition manifests itself as a redistribution of the magnetocrystalline anisotropy axis (both in strength and direction) from the austenite to the martensite phase. Therefore, a fundamental question arises: what is the nature of the magneto-elastic coupling in these alloys and to what extent does it drive the structural transformation from the high-temperature, higher symmetry austenite phase to the low-temperature lower symmetry martensite phase? In the present study, through the development of a simple technique called "magnetic transition spectra" (MTS) to study temperature-dependent domain dynamics, as well as other experimental results, it is shown that the evolution of the micromagnetic structure is enslaved to and follows the structural transformation in these alloys. The MTS method is simple and versatile, and can also be used to study other magnetic transitions, such as the onset of exchange anisotropy in ferromagnetic-antiferromagnetic systems, the phenomenon of brittle-to-ductile transition in structural materials, and pressure-induced phase transitions.

II. EXPERIMENTAL DETAILS

Different off-stoichiometric {100} $Ni_{2+x}Mn_{1-x}Ga$ Heusler alloy single crystals as well as Fe−30 at % Pd single crystals were investigated. The single crystals were grown by the modified Bridgeman method and crystal orientation was determined by the Laue back-reflection method. Prior to the experiments, the samples were mechanically polished, followed by chemical etching to remove the strained layer caused by polishing. The transformation temperatures were measured using a differential scanning calorimeter (DSC). Note that DSC measurements were made using a commercial stage from Linkam (DSC 600) that allows DSC measurements with simultaneous *in situ* optical observations of the structural changes and automated capture of the micrographs. While this stage does not match the resolution of the traditional calorimeters, it is very effective in directly correlating structural changes with DSC output, which is otherwise not possible in traditional calorimeters. However, the signal to noise ratio and resolution was sufficient to discern

even the Curie transition at elevated temperatures in these alloys.

The temperature-dependent evolution of the micromagnetic structure was studied using the high-resolution interference-contrast-colloid (ICC) technique. The ICC method[9] and micromagnetics of FSMAs are discussed in detail elsewhere.[5–8] Briefly, the ICC method employs a colloidal solution to decorate the microfield on a magnetic surface, similar to the versatile Bitter method.[10] However, the technique differs in the manner in which the colloid decorated microfield is detected. In the Bitter method, a problem in contrasts develops in the bright-field or the dark-field mode due to backscattering by particles and the various surfaces between the objective lens and the specimen, which results in an overall loss of resolution. Instead, the ICC method uses a Nomarski interferometer to detect the surface microfield distribution. The magnetic microfield on a magnetic surface causes local variation in the density of colloid particles (average colloid particle size is 7 nm), thereby delineating the domain structure. This microfield is detected by polarization interferometer optics, which detects any unevenness at the nanometer scale and reveals domain structure with a pronounced three-dimensional effect and at a high resolution limited only by the resolution of the microscope. In this manner, the micromagnetic structure is directly observed superimposed on the microstructure of the sample as a function of temperature. In order to prevent freezing of the (water-based) ferrofluids, an oil-based ferrofluid was used, which remains stable from 70 °C to −35 °C. Observations were made by placing the samples in a commercially available precision heating and cooling stage from Linkam (THMSE 600) with an accuracy of ±0.1 deg.

Technique of magnetic transition spectra

The structural transformation in FSMAs is martensitic, which owing to its displacive and diffusionless nature proceeds at a speed approaching the transmission of elastic waves in a solid, modified (and slowed) by an appropriate damping factor and softening of the elastic constants in the premartensitic state.[11–13] Accompanying the martensite transformation in FSMAs is a reconfiguration of the micromagnetic structure. Therefore, a suitable method is required to provide simultaneous real-time information on both transitions. Whereas the martensitic transformation can be observed directly in an optical microscope using, say, a Nomarski interferometer, simultaneous monitoring of the high-speed magnetic transition using established techniques (such as the polar Kerr effect, magnetic force microscopy, Bitter method, or the ICC method) proved to be too cumbersome and/or slow or inconclusive. This is especially true when the two different transitions occur at different speeds and have to be followed simultaneously as a function of temperature in a sample contained in the protective environment of a heating/cooling stage. Therefore, a simple method was developed, which we refer to as the magnetic transition spectra (MTS) method.

The MTS method is an electronic method to monitor the change in micromagnetic structure as a function of temperature.[7,14] It is based on the same principle upon which the well-known and established Barkhausen method is based,[15] namely, Faraday's law: voltage ξ induced in a pickup coil is proportional to the rate of change of flux with time $\xi = -d\Phi/dt$ in a sample; $d\Phi$ is the flux change over a time interval dt. Whereas the Barkhausen method generates a spectrum of voltage spikes by placing a pickup coil next to a ferromagnetic sample and cycling the sample in an applied magnetic field (see, for example, Ref. 16), the MTS method generates a spectrum of voltage by *sweeping the sample across the transformation temperatures* instead of applying any magnetic field. As a result of phase transformation, either during forward or reverse martensitic transition, change in flux occurs in the sample. The resulting spectrum of voltage spikes as a function of temperature is recorded by an adjacent pickup coil. The MTS method is especially well suited for studying magnetic transitions in FSMAs because the local change in flux occurs over short intervals of time, which in turn leads to a high output signal.

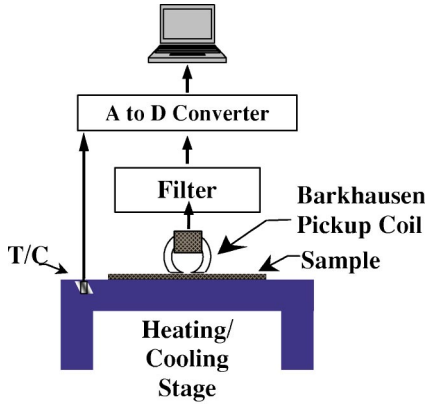

FIG. 1. Schematic of the experimental setup for acquiring the magnetic transition spectrum. (T/C: thermocouple).

The experimental setup used in the MTS method is the same as that for the Barkhausen method.[16] However, unlike the Barkhausen method, where an energizing coil is used to generate a magnetic field to sweep the sample, a heating/cooling stage is used in the MTS method, as shown schematically in Fig. 1. The MTS signal pickup coil is a specially designed and optimized miniature surface probe fabricated out of an insulating ferrite core. Its output is bandwidth limited by a bandpass filter to a range of 1–10 kHz. The pickup coil is a miniature probe in the form of a hemispherical ring 2–3 mm in diameter, 1 mm thick, and having 50 encircling coil turns. The sample is attached to the probe and placed in a commercial temperature stage (Linkam, England) that is capable of heating and cooling the sample from 77 to 873 K to within ±0.1 °C. The heating/cooling stage is fully automated and interfaced with an image frame grabber (Linkam) and a synchronized high-speed data acquisition card. Furthermore, the experimental setup acquires and labels all images and data automatically following the execution of a preprogramed heating/cooling cycle. The software operating the stage and acquisition card also has the ability to embed important experimental information (temperature, heating/cooling rate, etc.) directly on the recorded optical micrographs, which themselves are collated and numbered

automatically by the software. This degree of automation ensures unambiguous correlation between the microstructure and the acquired MTS spectrum as a function of temperature. The samples were cooled/heated from rates as low as 0.1 °C/min to 30 °C/min. The MTS spectra were found to be independent of the measured heating/cooling rates because the transformation occurs at speeds much faster than the temperature scans. Moreover, the transition temperatures were found to be unaffected by the presence of the miniature pickup coil lying adjacent to the samples. As the sample is cooled or heated across its critical transformation temperatures, the signal from the MTS coil is digitized by the computer and analyzed subsequently.

III. RESULTS AND DISCUSSION

Figure 2 shows the DSC curves of a Ni–Mn–Ga sample, which delineates the critical transformation temperatures for both forward and reverse martensitic transition; see Refs. 17–19. As seen from Fig. 2, and also confirmed by *in situ* optical observations, the martensite start M_s and finish M_f temperatures are −19.3 °C and −19.6 °C, respectively, and the austenite start A_s and finish A_f temperatures are −13 °C and −12.7 °C, respectively; the sample had a Curie temperature of 92 °C. DSC curves from a smaller portion of the same sample between −10 °C and −40 °C are shown in the inset in Fig. 2. The inset shows no other transformation except for that shown in Fig. 2. Figures 3(a)–3(l) and Figs. 4(a)–4(i) show, respectively, the optical micrographs that were simultaneously acquired *in situ* during the DSC measurements for cooling and heating. The field of view in the microscope was only slightly smaller than the sample size, and these figures directly show the narrow transformation range (0.3–0.4 °C) for the sample. Such a narrow transformation temperature spread was achieved through painstaking selection of a highly homogeneous sample. It was cut from a bar of approximate dimensions $10\times0.8\times0.5$ mm. Energy dispersive x-ray spectroscopy (EDXS) of this bar showed a slight composition variation from one end to the other, which manifested in a dispersion of several degrees in critical temperatures of the martensite transformation. To reduce this unwarranted dispersion, a smaller sample was carefully cut from this long bar, whose final dimensions were approximately, $2\times0.8\times0.5$ mm. EDXS on this sample showed no measurable composition variation across its dimensions. The composition of this homogeneous sample was $Ni_{54.35}Mn_{23.18}Ga_{22.47}$. Both MTS and DSC measurements were performed on the same homogeneous sample. Chemical homogeneity and extreme care to handle the sample (using plastic tweezers) were necessary to ensure a narrow spread in the transformation temperatures. For example, we have found that handling the samples even with a metal tweezers can generate enough permanent strains during gripping to cause mechanical inhomogeneity and a measurable broadening of the transition temperatures.

Detailed temperature-dependent micromagnetic studies show that the high-temperature face-centered cubic (fcc) phase exists in a large single magnetic domain state spanning several thousand microns, and this was a common feature for both Ni–Mn–Ga and Fe–Pd alloys.[6–8] The martensite transition results in the transformation of the structurally and magnetically homogeneous high-temperature austenite phase into the heterogeneous low-temperature martensite phase. Structurally, the "heterogeneity" refers to the formation of fine twins, which are differently oriented variants of the lower symmetry martensite phase. Magnetically, whereas the fcc phase has spatially well-defined magnetocrystalline anisotropy axes throughout the volume of the crystal, the direction of the magnetocrystalline anisotropy in the martensite phase varies from one twin plate to the other. This causes a micromagnetic reconfiguration from a single domain state in the fcc phase to a multiplicity of magnetic domains in the martensite phase. An example of the structurally and magnetically heterogeneous martensite state is shown in Fig. 5 for a Ni–Mn–Ga sample. Note that the micromagnetic structure in Fig. 5 is from a different sample and is shown solely to illustrate the multidomain micromagnetic structure of the transformed state. In Fig. 5, the magnetic domains can be seen confined within the martensite bands that run diagonally across the micrographs from left to right. Also note the presence of "interdomain" walls that traverse numerous thick bands. As discussed in detail elsewhere,[6] the domain structure in Fig. 5 is a result of a complex martensite structure, and can be explained by taking into account the fact that the thick martensite bands are not homogeneous entities but are in fact internally twinned.

Due to the high speed of the martensite transformation, a catastrophic or avalanche-like reconfiguration of the magnetic domain structure occurs in the crystal on passing from the single domain fcc phase to multidomain face-centered tetragonal (fct) phase. This gives rise to a spectrum of voltage spikes reflecting the dynamics of the magnetic transition. Figure 6(a) shows the acquired magnetic transition spectrum accompanying the martensite transformation in the Ni–Mn–Ga sample whose DSC curve is shown in Fig. 2. As shown in Fig. 6(a), the MTS consists of a very large number of voltage spikes reflecting the dynamics of micromagnetic reconfiguration. The inset in Fig. 6(a) is a magnified view of the acquired MTS spectrum, which clearly shows the avalanche-like distribution of the induced pulses. Previously, we have used a "jumpsum" method to analyze and interpret voltage spectra (Barkhausen spectra) in ferromagnetic materials.[16,20,21] The jumpsum analysis method is well suited because, instead of assigning an average or mean value to a given spectrum, it expresses the acquired signal in terms of the profile of the spectrum. Thus, with respect to Fig. 6(a), one of the signal parameters extracted from the MTS is called the jumpsum JS, which is simply the running total of all the voltage jump heights, as shown in Fig. 6(b)—the reverse *S* curve. The *i*th value of JS is equal to the sum of all preceding voltage jumps $\Sigma_{i=1}^{i=l}\xi_i$ up to that temperature on cooling. The inset in Fig. 6(b) is a magnified view of a portion of the JS curve, which shows that the JS curve is in fact made up of a large number of jumps or steps. The M_s and M_f temperatures for this alloy were measured using both calorimetery and optical observations, and are also indicated in Fig. 6. As seen from Fig. 6(b), the JS value is zero above the M_s temperature and rises to a saturation value within a narrow temperature interval $\Delta T=T_s-T_f$ of 1.5 deg [the essen-

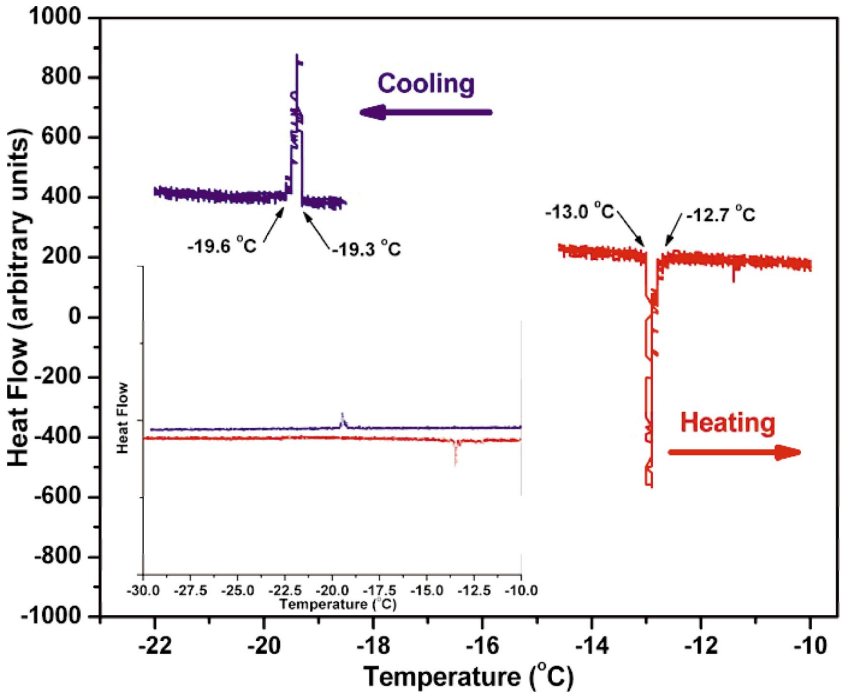

FIG. 2. (Color) DSC curves for the forward (cooling) and reverse (heating) martensite transformation in a Ni–Mn–Ga sample. Inset shows the DSC from a smaller portion of the same sample and taken in a broader temperature range from −10 °C to −30 °C.

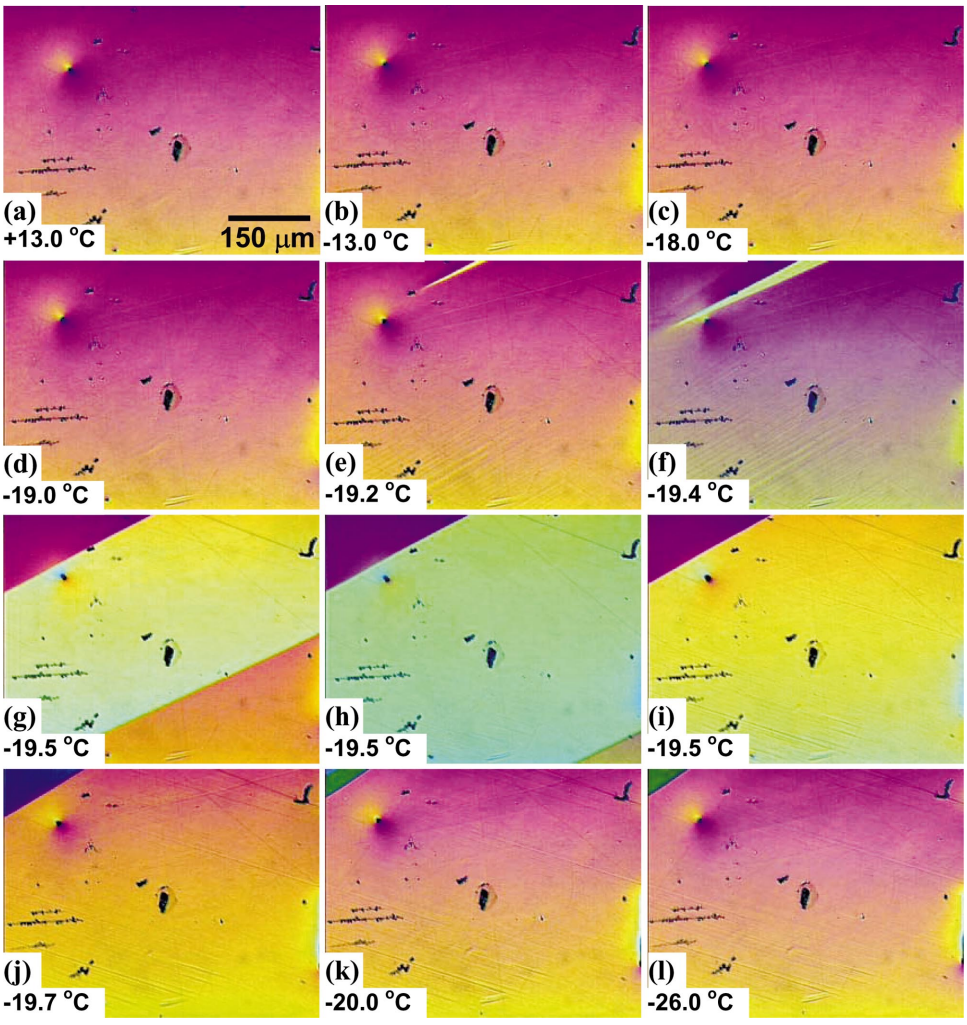

FIG. 3. (Color) (a)–(l) Optical micrograph taken *in situ* with the DSC cooling cycle in Fig. 2 showing the narrow temperature range for the martensite transformation. The field of view is only slightly smaller than the actual sample size.

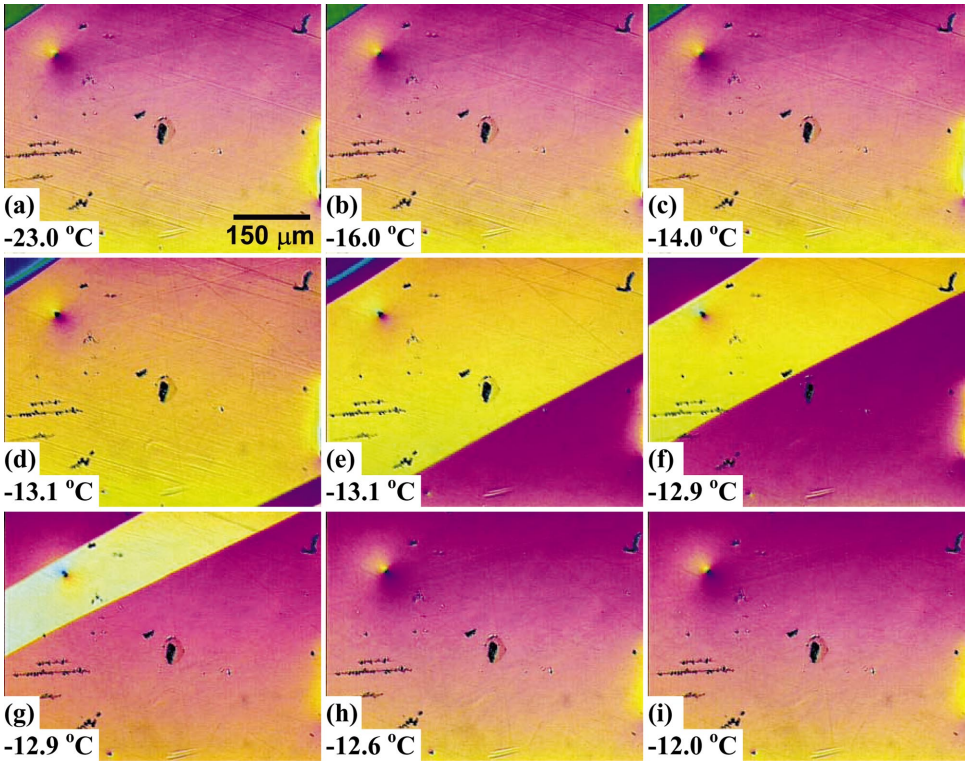

FIG. 4. (Color) (a)–(i) Optical micrograph taken *in situ* with the DSC heating cycle in Fig. 2 showing the narrow temperature range for the reverse martensite transformation. The field of view is only slightly smaller than the actual sample size.

tially zero initial slope of the JS curve in Fig. 6(b) is due to small magnitude of jumps at the start of the transformation]. In other words, *the structural transition precedes the micromagnetic reconfiguration on cooling*. Another parameter derived is called the jumpsum rate, JSR, which is simply the rate at which flux is being emitted by the sample.

A composite of JS and JSR curves for both cooling and heating cycles for the Ni–Mn–Ga sample is shown in Fig. 7; similar curves were obtained for the Fe–Pd alloys. [Note that the JS and JSR curves in Fig. 6 and 7 start from right to left for cooling, and from left to right for heating.] The noteworthy feature of JS and JSR curves in Figs. 6 and 7 is the clear indication that during cooling, the magnetic transition occurs after the structural transformation, whereas on heating the magnetic transition is complete before the structural transition begins. In other words, the sequence of structural and magnetic transitions was found to be as follows: *Cooling: structural transition→magnetic transition; Heating: magnetic transition→structural transition.*

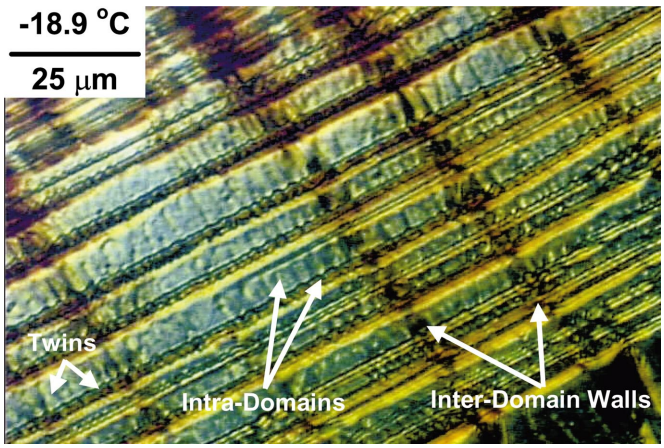

FIG. 5. (Color) Micrograph showing the magnetic domain structure of the fct martensite in a Ni–Mn–Ga sample. Note the presence of domains within the bands as well as interdomain walls spanning several bands. This micrograph was taken from a different Ni–Mn–Ga sample.

The precedence of the martensite transition over magnetic transition, say, during cooling, is further highlighted in Fig. 8, which shows a collage of micrographs that were acquired *in situ* with the MTS measurements and overlaid on the JS curve of Fe−30at %Pd alloy. Unlike the Ni–Mn–Ga system, where the martensite transition occurs by the formation of very fine twins through the motion of a single interface across the surface of the sample, martensite transformation in the Fe–Pd alloy occurs by the abrupt, burst-like transformation of large volumes of the crystal into thick twin bands. This jerky and burst-like mode of transformation makes it easier to further illustrate the relative sequence of magnetic and structural transitions. The collage in Fig. 8 shows that *the formation of each set of twin bands leads to a sharp increase in the* JS *value*. The micrographs in the collage in Fig. 8 were acquired *in situ* with MTS measurements, and they show unambiguously the sequence of magnetic and structural transitions. The inset in Fig. 8 shows the JSR curves for Fe–Pd during cooling and heating. It is interesting to note the similarities of the JSR curves in the insets of Fig. 7 and 8 with curves obtained during magneto-caloric measurements by Marcos *et al.*[18] Such a comparison is worthwhile for the future as it could provide insight into the interplay between magnetic, elastic, and caloric effects occurring during the transformation in these alloys.

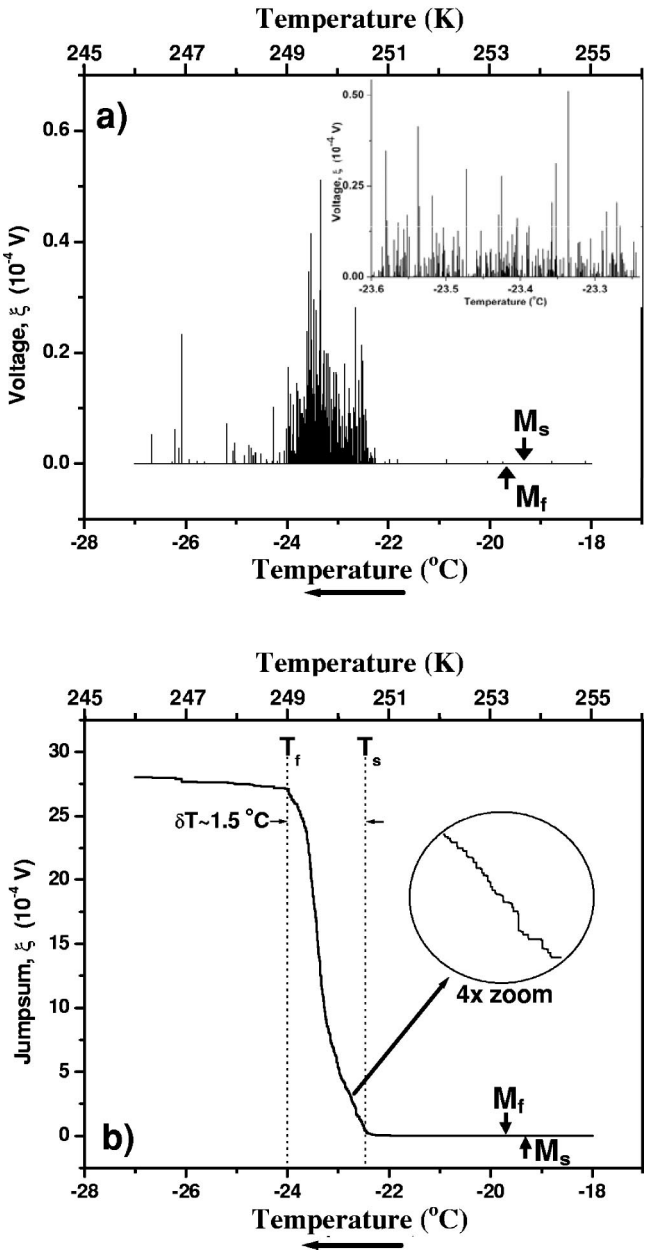

FIG. 6. (a) Magnetic transition spectrum for a Ni–Mn–Ga sample on cooling from a sample whose DSC curve is shown in Fig. 2. Note that the jumps occur below the martensite transformation. (b) The JS curve corresponding to the MTS in (a). The inset in (a) is a magnified view of the MTS over a small temperature interval, and shows the avalanche-like behavior of the jumps. The inset in (b) is a magnified view, which shows that the JS curve consists of a large number of jumps.

As a visual aid, the temperature-dependent evolution of the micromagnetic structure with respect to the structural transformation in Fe–Pd alloy is shown in a movie that is submitted as a supplementary material along with this manuscript; see Ref. 22 to access this movie from AIP's Electronic Physics Auxiliary Publication Service (EPAPS). The movie shows real-time, temperature-dependent evolution of the microstructure and the micromagnetic structure in an Fe–Pd alloy. The movie starts with the sample in the single domain fcc phase above the martensite temperature. On cooling, the reconfiguration of the magnetic domains can be clearly seen lagging behind the martensite transformation. Due to the abrupt martensite transformation, the magnetic structure finds itself incongruous with the new boundary condition imposed by the formation of the twin. The ensuing motion and self-accommodation of the magnetic domains into a micromagnetic structure that is consistent with the martensite structure is clearly evident in the movie. On heating, the magnetic domains can be seen moving and coalescing together well before the reverse martensite transformation begins.

The avalanche-like behavior (as a general phenomenon) and avalanches in the Barkhausen spectrum due to an applied magnetic field are well studied.[23–31] In particular, Vives *et al.*[32] have studied acoustic emissions in a *nonmagnetic* Cu–Zn–Al shape-memory alloy. They have observed avalanche-like behavior associated with the formation of *nonmagnetic* martensite plates. In addition, Hardy *et al.*[33] have shown the time-dependent evolution of magnetization in manganite in a constant field. The conclusion of the present study is that the magnetic transition is enslaved to the structural transition. Since MTS in the present study was taken in the *absence* of any applied magnetic field, avalanche-like behavior in the MTS signal seems to show an enslaved magnetic signal arising from the avalanche-like behavior of martensite plates. While statistical analysis of the spectra for jump amplitudes is beyond the scope of this work, these observations provides an interesting framework for further study of the athermal and time-dependent nature of martensite transformation in ferromagnetic shape-memory alloys in the future.

Finally, the MTS method is simple to implement and can be used to study other magnetic phase transitions driven by *any* external influence that would cause an abrupt change in the micromagnetic state of the sample (for example, change in temperature, pressure, etc.). For example, we have successfully applied this method to study the onset of coupling in exchange anisotropy ferromagnetic films coupled to an antiferromagnetic substrate, using the Co–CoO system.[34] Other potential applications of MTS include fundamental investigation of ductile to brittle transition in ferromagnetic structural materials and pressure-induced phase transitions. One limitation of the method, however, is the upper temperature limit. While it is easy to implement the technique for low-temperature studies, it would need modifications, both in the probe design and signal processing, when the temperatures exceed 70–80 °C. Nonetheless, the MTS method could find applications in many fundamental investigations.

IV. CONCLUSIONS

In conclusion, the present study shows that the micromagnetic reconfiguration during structural transformation in FSMAs is completely enslaved to the structural transformation. The sequence of structural and magnetic transitions was

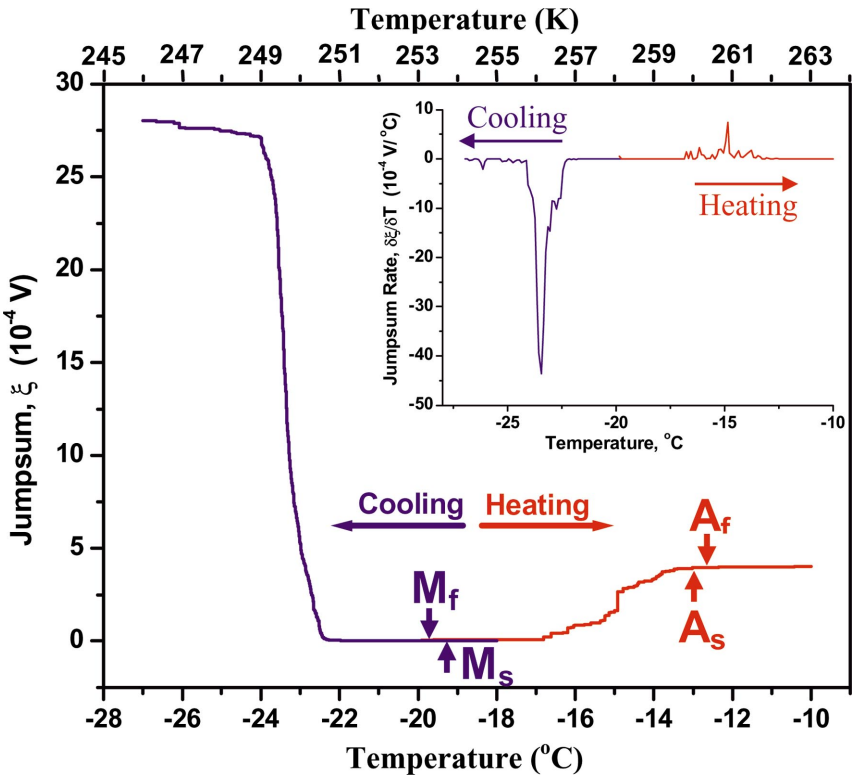

FIG. 7. (Color) Composite of JS and JSR curves for cooling and heating for a Ni–Mn–Ga sample. Note: For cooling the JS curve goes from right to left, whereas for heating the JS curve goes from left to right.

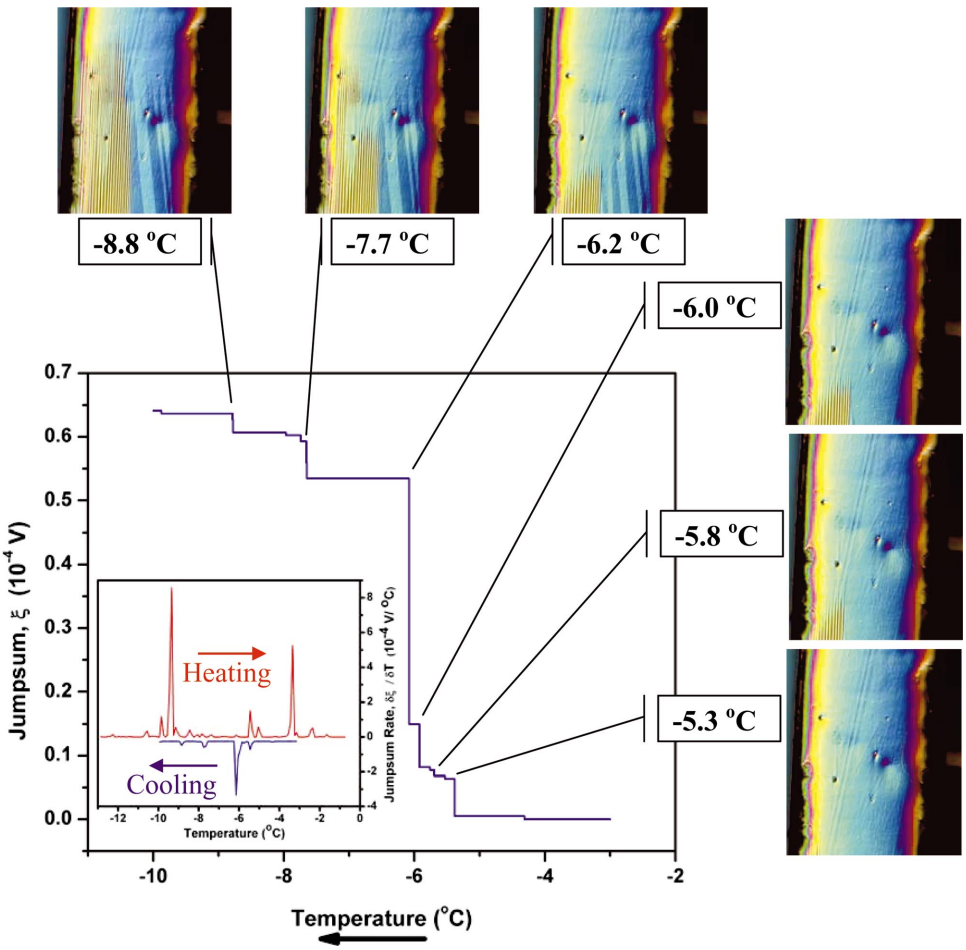

FIG. 8. (Color) Collage showing the JS curve for Fe−30 at %Pd sample and the corresponding change in microstructure responsible for each jump in the JS curve. The inset shows JS and JSR curves for cooling and heating.

found to be as follows: Cooling: structural transition followed by micromagnetic reconfiguration; Heating: micromagnetic reconfiguration followed by structural transition. The MTS method is simple and can be adapted to study other phenomena where an abrupt change in flux occurs, for example, due to change in temperature or pressure.

ACKNOWLEDGMENTS

This work was supported by the Department of Energy, Office of Basic Energy Science, Grant No. DE-FG02-01ER45906, and this support is gratefully acknowledged. The authors thank M. Wuttig for providing Fe–Pd samples.

*Corresponding author. Email address: hchopra@eng.buffalo.edu

[1] K. Ullakko, J. K. Huang, C. Kantner, R. C. O'Handley, and V. V. Kokorin, Appl. Phys. Lett. **69**, 1966 (1996).

[2] R. D. James and M. Wuttig, Philos. Mag. A **77**, 1273 (1998).

[3] V. A. Chernenko, E. Cesari, V. V. Kokorin, and I. N. Vitenko, Scr. Metall. Mater. **33**, 1239 (1995).

[4] F-X. Hu, B. G. Shen, and J-R. Sun, Appl. Phys. Lett. **76**, 3460 (2000).

[5] H. D. Chopra, C. Ji, V. V. Kokorin, Phys. Rev. B **61**, R14913 (2000).

[6] M. R. Sullivan and H. D. Chopra, preceding paper, Phys. Rev. B **70**, 094427 (2004).

[7] M. R. Sullivan, D. A. Ateya, S. Pirotta, A. A. Shah, G. H. Wu, and H. D. Chopra, in "Materials and Devices for Smart Systems," edited by Y. Furuya, E. Quandt, Q. Zhang, K. Inoue, and M. Shahinpoor, Vol. 785, MRS Fall 2003 Proceedings, Boston, MA (2004), p. 457.

[8] M. R. Sullivan, D. A. Ateya, S. J. Pirotta, A. A. Shah, G. H. Wu, and H. D. Chopra, J. Appl. Phys. **95**, 6951(2004).

[9] H. D. Chopra, D. X. Yang, P. J. Chen, H. J. Brown, L. J. Swartzendruber, and W. F. Egelhoff, Jr., Phys. Rev. B **61**, 15312 (2000).

[10] F. Bitter, Phys. Rev. **38**, 1903 (1931).

[11] H. D. Chopra and M. Wuttig, J. Phys. IV, Colloq. C8, supplement au J. Phys. III **5**, C8/157 (1995).

[12] S. Muto, R. Oshima, and F. E. Fujita, Acta Metall. Mater. **38**, 685 (1990).

[13] H. D. Chopra, Ph.D. thesis, University of Maryland (1993).

[14] H. D. Chopra, M. R. Sullivan, and L. J. Swartzendruber, U.S. Patent (Provisional), 27 August 2003, "Magnetic phase transition and magnetic structure characterization using modified Barkhausen effect and method of using the same."

[15] H. Barkhausen, Phys. Z. **20**, 401 (1919).

[16] H. D. Chopra, G. E. Hicho, and L. J. Swartzendruber, Mater. Eval. **59**, 1215 (2001).

[17] Our interest was simply to ascertain critical temperatures of the martensite transformation by an additional mean, in conjunction with MTS with *in situ* optical structural/micromagnetic studies. Unlike quantitative DSC, this did not require us to calibrate the DSC heat output to quantitatively make determination of heats of transformation. Hence, the DSC output is given in arbitrary units. This is a common practice in the literature when determination of critical temperatures is the only objective of interest. Several rigorous calorimetery studies have been done in the past, but it was not the focus of our study. References 18 and 19 describe detailed calorimetery studies on these alloys.

[18] J. Marcos, A. Planes, L. Mañosa, F. Casanova, X. Batlle, A. Labarta, and B. Martínez, Phys. Rev. B **66**, 224413 (2002).

[19] V. V. Khovailo, K. Oikawa, T. Abe, and T. Takagi, J. Appl. Phys. **93**, 8483 (2003).

[20] G. Kohn, G. E. Hicho, and L. J. Swartzendruber, U.S. Patent No. 5,619,135 (8 April 1997), "Steel characteristics measurement system using Barkhausen jump sum rate and magnetic field intensity and method of using same."

[21] L. J. Swartzendruber, G. E. Hicho, S. D. Leigh, H. D. Chopra, G. Adam, and E. Tsory, J. Appl. Phys. **81**, 4263 (1997).

[22] See EPAPS Document No. E-PRBMDO-70-090429 for accessing this movie, which shows the forward (cooling) and reverse (heating) martensite transformation and evolution of micromagnetic structure in Fe−30 at %Pd sample. The optical contrast in the movie during experiments was changed slightly for the heating cycle in order to distinguish it from the cooling cycle. A direct link to this document may be found in the online article's HTML reference section. The document may also be reached via the EPAPS homepage (http://www.aip.org/pubservs/epaps.html) or from ftp.aip.org in the directory /epaps/. See the EPAPS homepage for more information.

[23] J. P. Sethna, J. D. Shore, and M. Huang, Phys. Rev. B **44**, 4943 (1991), and references therein.

[24] S. Field, J. Witt, F. Nori, and X. Ling, Phys. Rev. Lett. **74**, 1206 (1995).

[25] W. Wu and P. W. Adams, Phys. Rev. Lett. **74**, 610 (1995).

[26] M. P. Lilly, P. T. Finley, and R. B. Hallock, Phys. Rev. Lett. **71**, 4186 (1993).

[27] J. Ortín *et al.*, J. Phys. IV **5**, 209 (1995).

[28] B. Gutenberg and C. F. Richter, Ann. Geofis. **9**, 1 (1956).

[29] J. P. Sethna, K. A. Dahmen, and C. R. Myers, Nature (London) **410**, 242 (2001).

[30] A. P. Mehta, A. C. Mills, K. A. Dahmen, and J. P. Sethna, Phys. Rev. E **65**, 046139 (2002).

[31] J. S. Urbach, R. C. Madison, and J. T. Markert, Phys. Rev. Lett. **75**, 4694 (1995).

[32] E. Vives, J. Ortín, L. Mañosa, I. Ràfols, R. Pérez-Magrané, and A. Planes, Phys. Rev. Lett. **72**, 1694 (1994).

[33] V. Hardy, A. Maignan, S. Hébert, C. Yaiele, C. Martin, M. Hervieu, M. R. Lees, G. Rowlands, D. M. K. Paul., and B. Raveau, Phys. Rev. B **68**, 220402(R) (2003).

[34] M. R. Sullivan and H. D. Chopra (unpublished).